Effects of Defining Realistic Compositions of the Ocular Melanoma on Proton Therapy

Keshazare Sh[1], Masoudi S F[2]*, S Rasouli F[3]

[1]MSc Student in Applied Nuclear Physics, Department of Physics, KN Toosi University of Technology, Tehran, Iran

[2]Associate Professor of Physics Department, Head of Nuclear Physics Group, Department of Physics, KN Toosi University of Technology, Tehran, Iran

[3]PhD Student in Applied Nuclear Physics, Department of Physics, KN Toosi University of Technology, Tehran, Iran

ABSTRACT

Background: Recent studies in eye plaque brachytherapy have shown a considerable difference between the dosimetric results using water phantom and a model of human eye containing realistic materials. In spite of this fact, there is a lack of simulation studies based on such a model in proton therapy literatures. In the presented work, the effect of utilizing an eye model with ocular media on proton therapy is investigated using the MCNPX Monte Carlo Code.

Methods: Two different eye models are proposed to study the effect of defining realistic materials on dose deposition due to utilizing pencil beam scanning (PBS) method for proton therapy of ocular melanoma. The first model is filled with water, and the second one contains the realistic materials of tumor and vitreous. Spread out Bragg peaks (SOBP) are created to cover a typical tumor volume. Moreover, isodose curves are figured in order to evaluate planar variations of absorbed dose in two models.

Results: The results show that the maximum delivered dose in ocular media is approximately 12-32% more than in water phantom. Also it is found that using the optimized weighted beams in water phantom leads to disturbance of uniformity of SOBP in ocular media.

Conclusion: Similar to the results reported in eye brachytherapy published papers, considering the ocular media in simulation studies leads to a more realistic assessment of sufficiency of the designed proton beam in tissue. This effect is of special importance in creating SOBP, as well as in delivered dose in the tumor boundaries in proton pencil beam scanning method.

Keywords

Proton therapy, Uveal melanoma, Dosimetry, SOBP, MCNPX

Introduction

Melanoma of the uveal layer (choroid, iris, ciliary body) is the most common primary intraocular malignant tumor in adults. These tumors can lead to blindness, loss of the eye, and even spreading to the optic nerve and brain. Although, for many years, the common type of treatment for ocular tumors was enucleation, other techniques such as radiotherapy have been replaced as the standard treatment to destroy the tumor as much as possible and to preserve the eye with useful vision simultaneously.

In 1966, Stallard proposed the treatment of uveal melanomas with radiation therapy [1]. The achievements in different radiotherapy methods also resulted in acceptable progresses in ocular treatment. As one of the most important types of radiotherapy of uveal melanomas, eye plaque

*Corresponding author: S F Masoudi
Associate Professor of Physics Department, Head of Nuclear Physics Group, Department of Physics, KN Toosi University of Technology, P.O. Box 15875-4416, Tehran, Iran
E-mail: masoudi@kntu.ac.ir

brachytherapy benefits of placing radioactive isotopes such as ^{125}I or ^{106}Ru on the sclera over the tumor. As an alternative powerful treatment method, external beam radiotherapy is based on the energy deposition of charged particles such as protons or helium ions in tissue. Other possible methods include stereotactic radiotherapy, transscleral or transretinal local resection, and transpupillary thermotherapy [2].

Of special interest method in treatment of uveal melanoma is proton therapy. The advantage of using proton beams in dose distribution in tissue and their effective role in treatment of tumors were proposed by Wilson in 1946 [3]. Constable and Koehler offered the treatment of intraocular neoplasms using low-energy proton beams [4]. This method presents more advantages in comparison with brachytherapy such as lower delivered dose to the optic nerve and less side effects such as vision loss after the treatment, as well as more reliable local tumor control. The local energy deposition of the proton beam leads to delivering precise and uniform dose to the tumor, and low dose to healthy tissues containing intraocular and orbital structures. Such a desirable performance in tissue which arises from physical characteristics of protons has made this method suitable for treating the small and deep tumors [5]. Moreover, the clinical results show about 97% local control and 90% eye retention rate after a 5 years follow up period [6]. Although the most ocular proton therapy is for choroidal melanomas [7], proton beams can also be used for treating other ocular tumors such as angioma, hamangioma, carcinoid lymphoma, conjunctival melanoma, metastic lesions, pediatric retinoblastoma (the most common malignant tumor of the eye in children), and macular degeneration [8].

It is found that the Monte Carlo is a powerful method for simulating transport of proton beams in materials, and producing a complete and precise set of data to carry out a treatment planning system [9-12]. The Monte Carlo based radiation transport codes model main related physical processes including coulombic energy loss, energy straggling, multiple coulomb scattering, elastic and inelastic scattering, nonelastic nuclear reactions and production of secondary particles [9].

Currently, one of the most attractive and advanced techniques in proton therapy is irradiation with a pencil beam of a few millimeters in diameter, named Pencil Beam Scanning (PBS) [13-15]. PBS can be defined as the act of moving a proton beam for the purpose of spreading the dose deposited by a beam throughout the target volume. Improvement of target volume coverage due to the improved geometric control of both lateral and distal fall-off in a single treatment field [16], and reduction of the secondary particles production which are unavoidable due to the proton interaction with range shifter materials in the nozzle [17], are the most important advantages of PBS. In addition, in this method, individual and narrow Bragg peaks can be delivered in three dimensions throughout the target volume. There are a variety of ways for moving the beam across the target such as scanning by mechanical motions, scanning by magnetic field variation to bend the beam trajectory, or combinations of these two methods [18].

In simulation studies for treatment purposes, it is common to use a simulated water filled phantom for transporting proton beam interactions. However, recent studies in brachytherapy show that defining the realistic materials of the eye and their compositions have considerable effects on dosimetric results [19, 20]. In spite of this fact, using the realistic eye materials in proton therapy is neglected in the related literatures [21, 22].

The presented work deals with the study of the effect of defining realistic compositions of the ocular melanoma in proton therapy. The method is based on irradiation of weighted proton pencil beams with different energies to a simulated water filled eye phantom, and to a phantom with realistic compositions in order

to cover the tumor area. Besides, the spread out Bragg peaks are created to extend the pristine narrow peaks to the desired target volume. The dosimetric results reveal the effect of defining realistic compositions in simulation studies for proton therapy. The Monte Carlo code, MCNPX is used to perform these simulations.

Materials and Methods

In the presented work, two models are simulated as eye phantom. These phantoms consist of a sphere with 1.2 cm radius as the human eye, with a tumor located at the corner. The tumor is modeled as a segment of a sphere with radius of 1 cm. This geometry is similar to the most common choroidal uveal melanoma [20]. A schematic figure of the simulated phantom is shown in figure 1.

In order to study the significance of using realistic tumor materials in simulations, two different set of materials are used. In the first model, the eye phantom is filled with water, as well as the tumor. This model is named "water phantom", and is the model which is used in the eye proton therapy simulation studies up to now. In the second model, the tumor is filled with the realistic material and the other part of the eye sphere is filled with vitreous, which is a thick, transparent substance that fills the center of the eye. It is composed mainly of water and comprises about 2/3 of the eye's volume, giving it form and shape. We have used the realistic compositions of the tumor and vitreous presented in table 1, which are reported in recent published work by Lesperance *et al*. [20].

In addition of studying the proton therapy in eye and water phantom, we have investigated the effects of defining realistic materials on spread out Bragg peak (SOBP). SOBP can be created by adding different Bragg curves with appropriate weighting factors to provide a flat dose distribution in desired volume. Mathematically this method can be described as follow [18]:

$$SOBP(R,d) = \sum_{(i=1)}^{N} \omega_i PP(R_i,d) \quad (1)$$

where $PP(R_i,d)$ is the pristine Bragg peak with range R_i, ω_i is the relative contribution of i-th peak to the $SOBP$, N is the number of added peaks, and $SOBP(R,d)$ is the resulting spread-out depth–dose curve with range R. The weights are optimized to form an ideal,

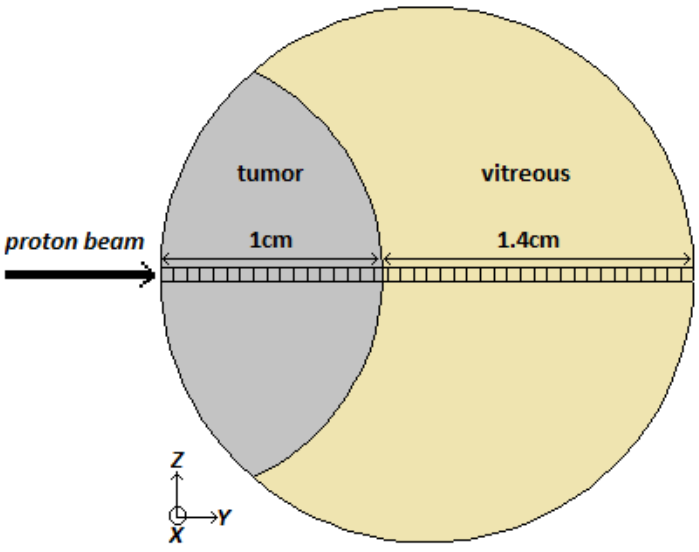

Figure 1: A schematic figure of the simulated eye phantom with a tumor located at the corner of the eye. The rectangular voxels are considered for dose calculation in depth direction.

Table 1: Elemental compositions of materials which are used in our simulation study. The data of vitreous and tumor are taken from Lesperance *et al*.'s work [20].

		Material compositions		
		Vitreous	Tumor	water
Elemental mass fraction	H	0.1109	0.0940	0.1119
	C	-	0.2120	-
	N	-	0.0560	-
	O	0.8804	0.6150	0.8881
	Na	0.0038	0.0025	-
	P	-	0.0051	-
	S	-	0.0064	-
	Cl	0.0045	0.0039	-
	K	0.0003	0.0051	-
Density (gr cm^{-3})		1.0071	1.040	1

presumably uniform, dose to the desired target volume. A typical created *SOBP* is shown in figure 2.

In the presented work, a monoenergetic and monodirectional proton source is located in front of the tumor. For the tumor location of our choice, rotating of the eye by patient moves the tumor toward the beam path. It will results in delivering dose to tumor and sparing other healthy tissue such as iris. Considering this fact, the proton beams are simulated to direct parallel to the y-axis so that the tumor is the first structure which protons see. Evidently, the more proton energies result in more penetration in tissue. Considering this fact, the proton energies are chosen so that the Bragg

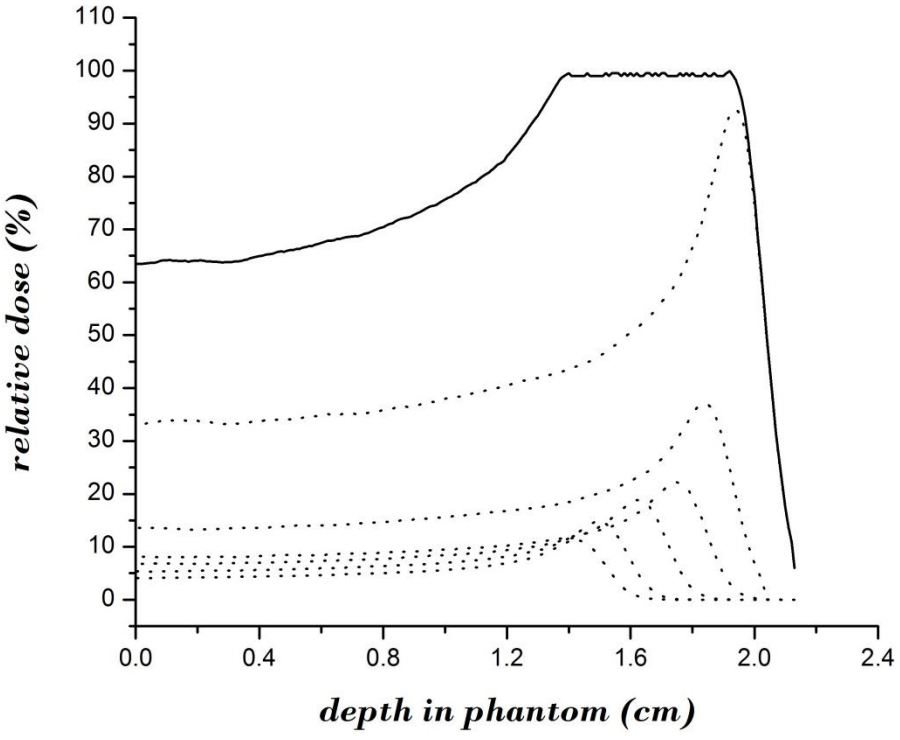

Figure 2: A typical created SOBP with subplot weighted Bragg peaks.

peaks cover the desired volume. The energies range from 22 to 32 MeV in 21 steps, and two different SOBPs are created in both mentioned models.

The dose is tallied as a function of depth (in y direction) in $0.1\times0.1\times0.1\ mm^3$ rectangular voxels. This method enables us to evaluate the performance of the protons in tissue in the direction parallel to the beam axis, naming depth-dose curves. Also, dose distributions are shown by means of isodose curves in two simulated models, to estimate planar variations in absorbed dose in phantoms. In order to create the isodose curves, the whole phantom is divided in voxels with mesh tally to show a diagram of depth dose measurement at various positions in which points of equal dose throughout the beam are joined together. Isodose curves can be used to evaluate the two dimensional dose distributions in a simulated model by irradiation of interested beam.

The simulations and dose evaluations presented in this work are carried out utilizing the MCNPX Monte Carlo code.

Results and Discussion

Depth-Dose curves and Bragg peaks

As mentioned earlier, the more proton energy results in more penetration in tissue, and the beam designer should consider appropriate proton energies in order to cover the whole tumor volume. In the presented section, proton pencil beams with different energies are irradiated to two eye models described in previous section, and the resultant Bragg peaks and depth-dose curves are calculated. As an example of the performance of protons in depth of two models, Bragg curves corresponding to two typical energies are shown in figure 3.

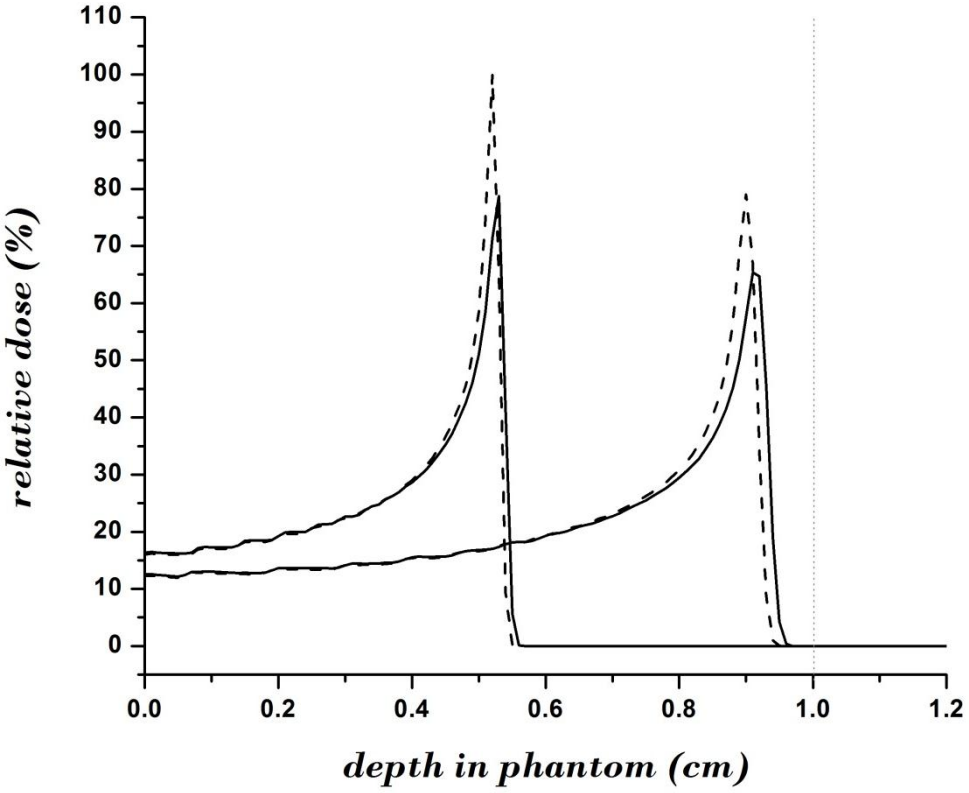

Figure 3: A profile of depth-dose curves due to the irradiation of two typical proton pencil beams to the water phantom (solid lines) and ocular media (dashed lines) which are described in Materials and Methods. The 31 *MeV* and 23 *MeV* proton beams are corresponding to the peaks which are formed in the more and less depths, respectively.

As can be seen, for a specific energy, the protons penetrate more in water, while deposit less dose in comparison to ocular media. Based on the dosimetric results, the maximum delivered dose in ocular media differs from those of water phantom by as much as 12-32%. Moreover, the difference between the depths which Bragg peaks occur is of special importance in the boundary of tumor and healthy tissue. In other words, if one determine the appropriate proton energy to fall a Bragg peak in the deepest part of the tumor volume (apex of tumor) based on the simulations in a water phantom, the apex will not receive this dose in realistic media. This arises from the lower penetration of beam in realistic ocular media. Considering this effect can be vital in tumors with small volume such as uveal melanoma. Similar to the same results reported in recent brachytherapy related published papers [19-20, 23], our simulations exhibit that defining realistic materials changes the dosimetric results in proton therapy.

Spread Out Bragg peak and weighting factors

It is well known that a strictly monoenergetic proton beam is unsuitable for cancer treatment due to the longitudinally narrow peak. Rather, it is necessary to 'spread out' the Bragg peak to deliver uniform dose within the target volume, by providing a suitably weighted energy distribution of the incident beam [24]. This section aims to investigate the effect of defining realistic media on uniformity of delivered dose to tumor. The method is based on multiplying appropriate optimized weighting factors in pristine Bragg curves to cover the extended tumor target volume in each depth with the required dose in both designed models (See eq. 1). The optimized weights for all utilized pencil beams irradiated in water phantom are presented in table 2, as well as the ocular media. The created SOBPs based on these weights are shown in figure 4. The effect of more penetration of pristine Bragg peaks in water phantom in comparison to ocular media can be seen in two SOBPs, too.

Table 2: The optimized weighting factors for utilized proton pencil beams in order to cover the desired volume with a uniform dose in two designed models.

Energy (MeV)	Eye weighting factor	Water weighting factor
22	0.1022	0.0961
22.5	0.1018	0.1027
23	0.1008	0.0988
23.5	0.1095	0.1016
24	0.1285	0.1165
24.5	0.1112	0.1219
25	0.119	0.1141
25.5	0.1308	0.1325
26	0.146	0.1358
26.5	0.1362	0.1383
27	0.1433	0.1405
27.5	0.1768	0.1683
28	0.1675	0.1648
28.5	0.1992	0.1907
29	0.1966	0.1948
29.5	0.2394	0.2296
30	0.2587	0.2645
30.5	0.3308	0.3016
31	0.396	0.3795
31.5	0.5002	0.4381
32	1.3503	1.64

In order to show the effect of defining realistic media in delivered dose in proton therapy simulations, the weighting factors optimized for water phantom are used to create a SOBP in ocular media. This procedure is equivalent to using the weighted proton pencil beams for a patient obtained from irradiation of the beams to a water phantom. The created SOBPs are shown in figure 5. Obviously, using this method leads to disturbance the uniformity of SOBP.

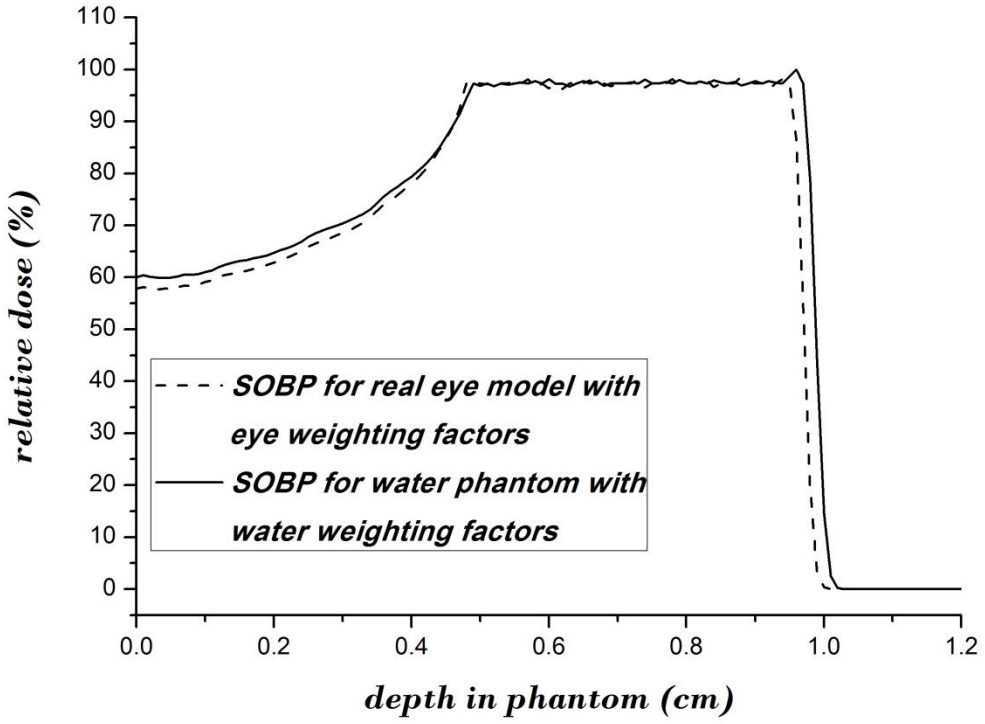

Figure 4: The created spread out Bragg peaks (*SOBP*) inside instance depths in water phantom and ocular media based on the optimized weighting factors reported in table 2.

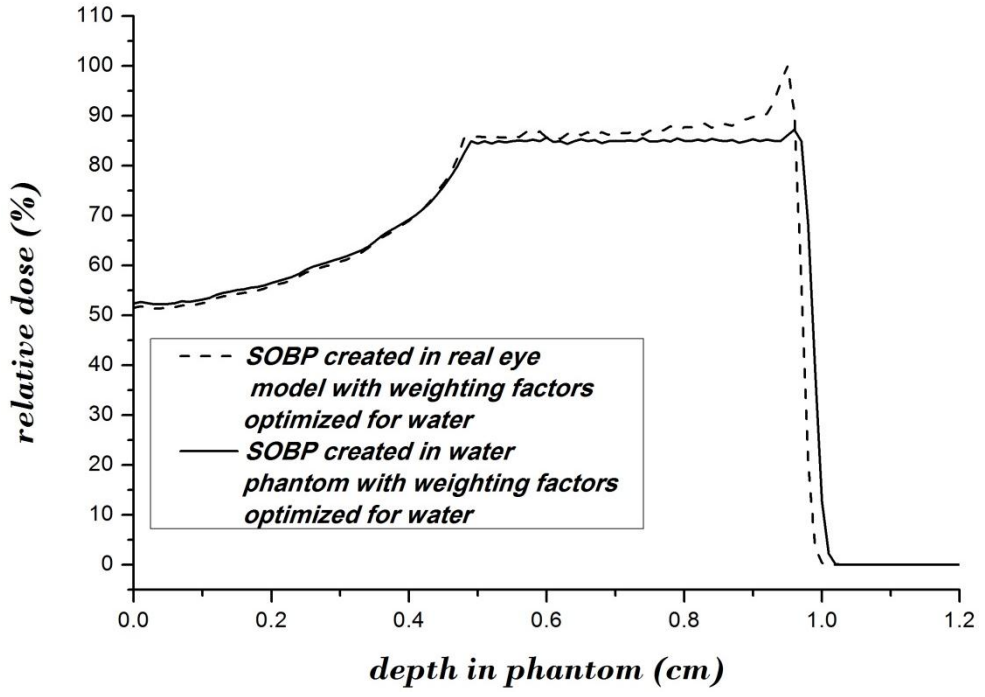

Figure 5: The created *SOBP* in instance depth of ocular media using the weighting factors which are optimized for water phantom (solid line), and the *SOBP* created in water phantom using the appropriate weighting factors for water (dashed line). See table 2.

Isodose curves in simulated eye models

The depth-dose curves reported in previous section show comparisons between the proton beam performances in realistic ocular media and water in the direction parallel to the beam axis. In order to evaluate the performance of the beams in two models, the results are figured in the form of isodose curves, which provide a demonstration of lines passing through points of equal dose. Figure 6 is an example of these curves corresponding to irradiation of 32 MeV proton beam to both models. These planar variations of deposited energy in two models not only agree with the results of depth-dose curves shown in figure 3, but also confirm with this known fact that proton therapy is a convenient method to protect surrounding healthy tissue as much as possible. In other words, the proton beam effect corresponds solely to the depths which are located in the direction of beam.

Conclusion

As a prominent method for treating localized small sized tumors such as uveal melanoma, proton therapy offers distinct advantages in comparison to the eye plaque brachytherapy. The presented work deals with the investigation of using realistic eye compositions on dosimetric results in proton therapy simulations. Two models of the human eye were simulated for dose calculations, one contains water to be used as "water phantom", and the latter contains vitreous and realistic tumor compositions. These models were subjected to the ir-

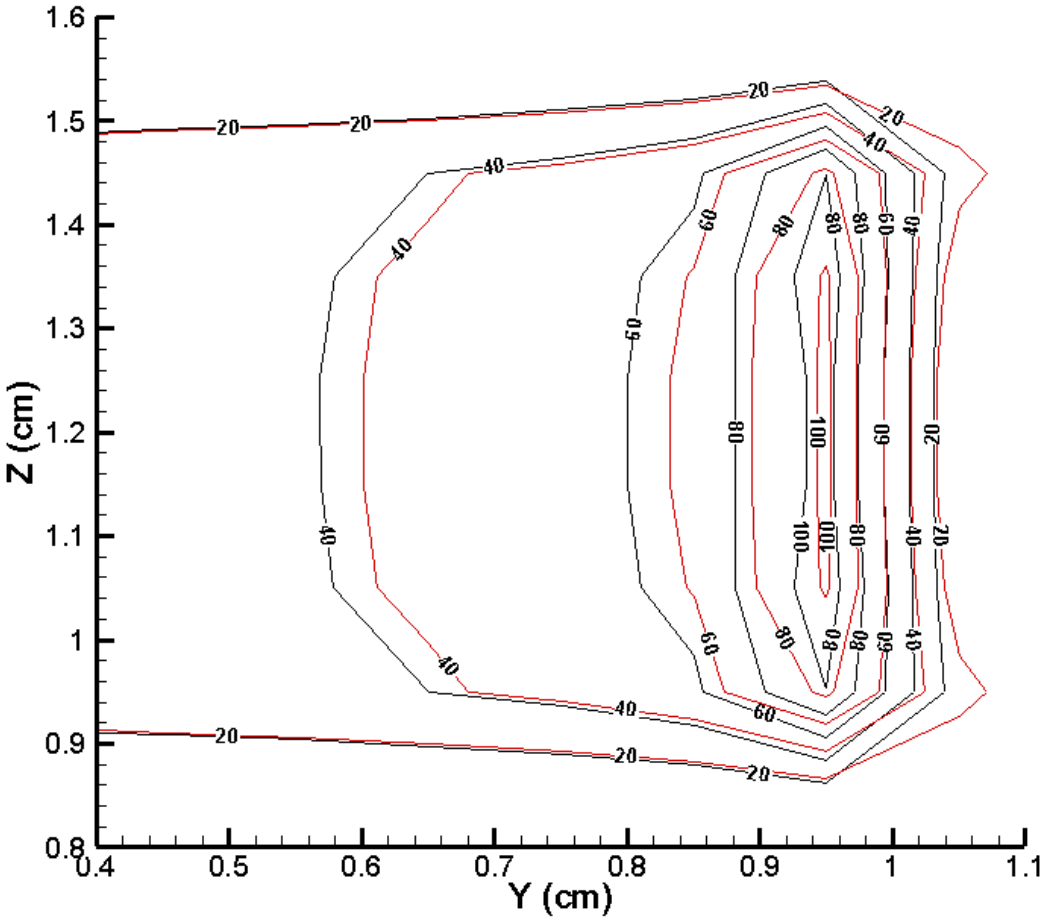

Figure 6: Relative isodose curves due to irradiation of a 32 *MeV* proton pencil beam to the water phantom (red curves) and ocular media (black curves). For better resolution, the horizontal axis is limited between 0.4 to 1.1 *cm*.

radiation of 22-32 MeV proton pencil beams to cover the desired target volume. The results show an incensement of 12-32% in maximum delivered dose in realistic ocular media in comparison to the water phantom. Moreover, the depth-dose curves show lower penetration of protons in realistic eye model. Considering the appropriate optimized weights required covering the extended tumor volume, SOBPs for two models were created. It was found that utilizing weighting factors calculated for pristine Bragg peaks in a water phantom for pristine profiles of realistic ocular media leads to disturbance the uniformity of SOBP. The study exhibits the effect of definition of a realistic ocular media in delivered dose to tumor boundaries, as well as in creating a flat and uniform SOBP in the desired volume.

Conflict of Interest

None

References

1. Stallard HB. Malignant melanoblastoma of the choroid. *Bibl Ophthalmol*. 1968;**75**:16-38. PubMed PMID: 5641363.
2. Damato B. *Ocular tumours: Diagnosis and treatment.* Oxford: Butterworth Heinemann. 2000. p. 250.
3. Wilson RR. Radiological use of fast protons. *Radiology*. 1946;**47**(5):487-91. doi: 10.1148/47.5.487. PubMed PMID: 20274616.
4. Constable IJ, Roehler AM. Experimental ocular irradiation with accelerated protons. *Invest Ophthalmol*. 1974;**13**(4):280-7. PubMed PMID: 4206547.
5. Damato B, Kacperek A, Chopra M, Campbell IR, Errington RD. Proton beam radiotherapy of choroidal melanoma: the Liverpool-Clatterbridge experience. *Int J Radiat Oncol Biol Phys*. 2005;**62**(5):1405-11. doi: 10.1016/j.ijrobp.2005.01.016. PubMed PMID: 16029800.
6. De Ruysscher D, Mark Lodge M, Jones B, Brada M, Munro A, Jefferson T, *et al*. Charged particles in radiotherapy: a 5-year update of a systematic review. *Radiother Oncol*. 2012;**103**(1):5-7. doi: 10.1016/j.radonc.2012.01.003. PubMed PMID: 22326572.
7. Slopsema RL, Mamalui M, Zhao T, Yeung D, Malyapa R, Li Z. Dosimetric properties of a proton beamline dedicated to the treatment of ocular disease. *Med Phys*. 2014;**41**(1):011707. doi: 10.1118/1.4842455. PubMed PMID: 24387499.
8. Newhauser WD, Burns J, Smith AR. Dosimetry for ocular proton beam therapy at the Harvard Cyclotron Laboratory based on the ICRU Report 59. *Med Phys*. 2002;**29**(9):1953-61. PubMed PMID: 12349914.
9. Newhauser W, Koch N, Hummel S, Ziegler M, Titt U. Monte Carlo simulations of a nozzle for the treatment of ocular tumours with high-energy proton beams. *Phys Med Biol*. 2005;**50**(22):5229-49. doi: 10.1088/0031-9155/50/22/002. PubMed PMID: 16264250.
10. Tourovsky A, Lomax AJ, Schneider U, Pedroni E. Monte Carlo dose calculations for spot scanned proton therapy. *Phys Med Biol*. 2005;**50**(5):971-81. doi: 10.1088/0031-9155/50/5/019. PubMed PMID: 15798269.
11. Herault J, Iborra N, Serrano B, Chauvel P. Monte Carlo simulation of a protontherapy platform devoted to ocular melanoma. *Med Phys*. 2005;**32**(4):910-9. PubMed PMID: 15895573.
12. Koch N, Newhauser W. Virtual commissioning of a treatment planning system for proton therapy of ocular cancers. *Radiat Prot Dosimetry*. 2005;**115**(1-4):159-63. doi: 10.1093/rpd/nci224. PubMed PMID: 16381705.
13. Grevillot L, Bertrand D, Dessy F, Freud N, Sarrut D. A Monte Carlo pencil beam scanning model for proton treatment plan simulation using GATE/GEANT4. *Phys Med Biol*. 2011;**56**(16):5203-19. doi: 10.1088/0031-9155/56/16/008. PubMed PMID: 21791731.
14. Grevillot L, Frisson T, Zahra N, Bertrand D, Stichelbaut F, Freud N, *et al*. Optimization of GEANT4 settings for Proton Pencil Beam Scanning simulations using GATE. *Nucl Instrum Methods Phys Res B*. 2010;**268**(20):3295-305. doi: http://dx.doi.org/10.1016/j.nimb.2010.07.011.
15. Gillin MT, Sahoo N, Bues M, Ciangaru G, Sawakuchi G, Poenisch F, *et al*. Commissioning of the discrete spot scanning proton beam delivery system at the University of Texas M.D. Anderson Cancer Center, Proton Therapy Center, Houston. *Med Phys*. 2010;**37**(1):154-63. PubMed PMID: 20175477.
16. Dowdell SJ, Clasie B, Depauw N, Metcalfe P, Rosenfeld AB, Kooy HM, *et al*. Monte Carlo study of the potential reduction in out-of-field dose using a patient-specific aperture in pencil beam scanning proton therapy. *Phys Med Biol*. 2012;**57**(10):2829-42. doi: 10.1088/0031-9155/57/10/2829. PubMed PMID: 22513726; PubMed Central PMCID:

PMC3373272.

17. Harvey MC, Polf JC, Smith AR, Mohan R. Feasibility studies of a passive scatter proton therapy nozzle without a range modulator wheel. *Med Phys*. 2008;**35**(6):2243-52. PubMed PMID: 18649454.
18. Paganetti H. *Series in Medical Physics and Biomedical Engineering; Proton Therapy Physics.* London: CRC Press, Taylor & Francis Group. 2012. p.704.
19. Asadi S, Masoudi SF, Shahriari M. The effects of variations in the density and composition of eye materials on ophthalmic brachytherapy dosimetry. *Med Dosim*. 2012;**37**(1):1-4. doi: 10.1016/j.meddos.2010.12.003. PubMed PMID: 21723111.
20. Lesperance M, Inglis-Whalen M, Thomson RM. Model-based dose calculations for COMS eye plaque brachytherapy using an anatomically realistic eye phantom. *Med Phys*. 2014;**41**(2):021717. doi: 10.1118/1.4861715. PubMed PMID: 24506608.
21. Randeniya SD, Taddei PJ, Newhauser WD, Yepes P. Intercomparision of Monte Carlo Radiation Transport Codes MCNPX, GEANT4, and FLUKA for Simulating Proton Radiotherapy of the Eye. *Nucl Technol*. 2009;**168**(3):810-4. PubMed PMID: 20865141; PubMed Central PMCID: PMC2943388.
22. Koch N, Newhauser WD, Titt U, Gombos D, Coombes K, Starkschall G. Monte Carlo calculations and measurements of absorbed dose per monitor unit for the treatment of uveal melanoma with proton therapy. *Phys Med Biol*. 2008;**53**(6):1581-94. doi: 10.1088/0031-9155/53/6/005. PubMed PMID: 18367789; PubMed Central PMCID: PMC4101899.
23. Dehghannia Rostami Z, Masoudi SF, Asadi S. Dosimetric Comparison of Water and Complete Eye Definition Phantoms for 125I and 103PD Brachytherapy Plaques. *Iran J Med Phys*. 2011;**8**(2):19-26.
24. Jette D, Chen W. Creating a spread-out Bragg peak in proton beams. *Phys Med Biol*. 2011;**56**(11):131-8. doi: 10.1088/0031-9155/56/11/N01.